Physics Letters A 380 (2016) 435–438

Contents lists available at ScienceDirect

Physics Letters A

www.elsevier.com/locate/pla

Vortices of a rotating two-component dipolar Bose–Einstein condensate in an optical lattice

Lin-Xue Wang [a,b], Biao Dong [b,c], Guang-Ping Chen [b,c], Wei Han [b], Shou-Gang Zhang [b], Yu-Ren Shi [a,*], Xiao-Fei Zhang [b,*]

[a] College of Physics and Electronic Engineering, Northwest Normal University, Lanzhou 730070, China
[b] Key Laboratory of Time and Frequency Primary Standards, National Time Service Center, Chinese Academy of Sciences, Xi'an 710600, China
[c] University of Chinese Academy of Sciences, Beijing 100049, China

ARTICLE INFO

Article history:
Received 18 July 2015
Received in revised form 26 September 2015
Accepted 9 November 2015
Communicated by R. Wu

Keywords:
Dipolar Bose–Einstein condensate
Optical lattice
Vortex sheet

ABSTRACT

We consider a two-component Bose–Einstein condensate, which consists of both dipolar and scalar bosonic atoms, in a confinement that is composed of a harmonic oscillator and an underlying optical lattice set rotation. When the dipoles are polarized along the symmetry axis of the harmonic potential, the ground-state density distributions of such a system are investigated as a function of the relative strength between the dipolar and contact interactions, and of the rotation frequency. Our results show that the number of vortices and its related vortex structures of such a system depend strongly on such system parameters. The special two-component system considered here opens up alternate ways for exploring the rich physics of dipolar quantum gases.

1. Introduction

Topological defects, such as the well-known quantized vortices and domain walls [1–6], appear in cross-disciplinary sub-fields of physics, and have attracted much interest of physicists. As a long-lived excitation, quantized vortex plays a very important role in understanding the topology of the order parameter and superfluidity.

Since the experimental realization of Bose–Einstein condensate (BEC) in dilute gases of alkali metals and hydrogen, it has became apparent that the isotropic *s*-wave interaction between the condensed atoms governs most of the observed phenomena [7–12]. However, recent experimental observations of BEC of ^{52}Cr ($6\mu_B$) [13–16], ^{168}Er ($7\mu_B$) [17,18], and ^{164}Dy ($10\mu_B$) [19] with μ_B being the Bohr magneton have shown that not only the static but also the dynamical properties depend strongly on the relative strength between dipole–dipole interaction (DDI) and contact interactions [20–24]. In addition, by using the Feshbach resonance, one can study the properties of a dipolar BEC with variable isotropic contact interaction [25–27]. Due to the unprecedented level of experimental control of the system's parameters, ultracold quantum gases provide us a completely new platform for exploring such topological excitations.

Very recently, the vortex structures and their interaction in a binary dipolar gas, wherein only one component possesses magnetic dipole moment, have drawn considerable attention [28–33]. Typically, in a most recent paper [28], Shirley et al. investigated the half-quantum vortex molecules of such a binary dipolar gas confined in a harmonic confinement; the anisotropic and long-range vortex in two-dimensional dipolar Bose gases was studied by Mulkerin et al. [29]. Furthermore, Zhang and his co-authors have studied the ground-state and rotational properties of such a system confined in concentrically coupled annular traps, and found that various ground-state phases and the related vortex structures can be obtained via a proper choice of the dipolar interaction and rotational frequency [30].

In real BEC experiments, ultracold atoms are always trapped by different external potentials. As far as we known, most of previous studies on a two-component dipolar condensate, which consists of both dipolar and scalar atoms, have been restricted to a free space or harmonic potential [34–36]. To our knowledge, there has been little work on the ground state densities of such a system confined in spin-dependent optical lattices [37], which is what we attempt to do in this work. In this paper, we carry out a detailed numerical analysis of the combined effects of DDI and rotation on the ground-state and rotational properties of such a two-component system confined in spin-dependent optical lattices. Our results

* Corresponding authors.
E-mail addresses: shiyr@nwnu.edu.cn (Y.-R. Shi), xfzhang@ntsc.ac.cn (X.-F. Zhang).

http://dx.doi.org/10.1016/j.physleta.2015.11.017
0375-9601/

show that the number of vortices and its related vortex structures of the system depend strongly on such system parameters.

The rest of this work is organized as follows. We formulate the theoretical model describing a two-component dipolar BEC in Sec. 2, in which we also briefly introduce the numerical method. In Sec. 3, we investigate the ground state properties of the system as a function of the relative strength between the dipolar and contact interactions, and of the rotation frequency. Finally, in Sec. 4, the main results of the paper are summarized.

2. The theoretical model and numerical method

We begin with a two-component bosonic cold atom gas in a confinement that is composed of a harmonic oscillator and an underlying optical lattice set rotation. For simplicity, we assume that the harmonic trapping frequencies satisfy $\omega_z \gg \omega_\perp$, then the condensates are pressed into a pancake. Within the framework of mean-field theory, the static and dynamical properties of such a system are governed by the so-called Gross–Pitaevskii (GP) equation, which can be written as [38,39],

$$i\hbar\frac{\partial\psi_i}{\partial t} = \Big(-\frac{\hbar^2\nabla^2}{2m_i} + V_{HOi} + \sum_{j=1,2} g_{ij}|\psi_j|^2 - \Omega_i L_z + \sum_{j=1,2} C_{dd}^{ij}\int U_{dd}(\mathbf{r})|\psi_j(r',t)|^2 dr'\Big)\psi_i, \quad (1)$$

where ψ_i is the wave function of the ith component ($i = 1, 2$), and m_i is the atomic mass. $L_z = -i\hbar(x\partial_y - y\partial_x)$ is the z component of the angular momentum, and Ω_i is the effective rotation frequency of component i. The intra- and inter-component coupling constants are given by $g_{ii} = 2\sqrt{2\pi}a_{ii}\hbar^2/ml_z$ and $g_{ij} = \sqrt{2\pi}a_{12}\hbar^2/m_R l_z$, with $l_z = \sqrt{\hbar/m\omega_z}$ and $m_R = m_1m_2/(m_1+m_2)$ being the axial harmonic oscillator length and the reduced mass, respectively. As discussed before, to further highlight the effects of DDI on a two-component system consists of both dipolar and scalar bosonic atoms, component 2 is considered to be "non-dipolar", leading to $C_{dd}^{22} = C_{dd}^{12} = C_{dd}^{21} = 0$ and $C_{dd}^{11} = \mu_0\mu^2/4\pi$ ($C_{dd}^{11} = d^2/4\pi\varepsilon_0$) for magnetic dipoles (electric dipoles), where μ_0 and μ being the magnetic permeability of vacuum and the magnetic dipole moment, respectively. Finally, we assume that the dipoles are polarized along the symmetry axis of the harmonic potential, and define a dimensionless quantity, $\varepsilon_{dd} = \mu_0\mu^2 m/12\pi\hbar^2 a_s$ with a_s being the three-dimensional s-wave scattering length, to character the relative strength between the dipolar and contact interactions. For the long-range and anisotropic DDI, U_{dd} can be written as,

$$U_{dd}(\mathbf{r}-\mathbf{r}') = \frac{1-3\cos^2\theta}{|\mathbf{r}-\mathbf{r}'|^3}, \quad (2)$$

where θ is the angle between the polarization direction and the inter-atom vector $\mathbf{r}-\mathbf{r}'$. In this work, the integral over the dipolar potential is evaluated in Fourier (momentum) space by a convolution identity requiring the Fourier transformation of the dipolar potential and the condensate density. By using the convolution theorem, the Fourier transform of the dipole potential, $U_{dd} = (4\pi/3)(3k_z^2/k^2 - 1)$, and integrating over the z direction, we arrive at the effective dipolar potential,

$$\Phi = C_{dd}^{11}\int U_{dd}(\mathbf{r}-\mathbf{r}')|\psi_1(r',t)|^2 dr' = \frac{4\sqrt{\pi}C_{dd}}{3\sqrt{2}a_z}\times\int\frac{d\vec{k}_r}{(2\pi)^2}e^{i\vec{k}_r\cdot\mathbf{r}}\tilde{n}(\vec{k}_r)h_{2D}(\frac{k_r a_z}{\sqrt{2}}), \quad (3)$$

where $\tilde{n}$ is the Fourier transform of $n(\mathbf{r}) = |\psi_1(\mathbf{r})|^2$, and $h_{2D}(k) = 2-3\sqrt{\pi}ke^{k^2}\mathrm{erfc}(k)$, with $\mathrm{erfc}(x)$ the complementary error function [28,30,40].

The external considered in this work is a combination of harmonic potential and spin-dependent optical lattices, which can be written as

$$V_{HOi}(x,y) = V_H + V_{OLi}, \quad (4)$$

where $V_H = \frac{1}{2}m[\omega_\perp(x^2+y^2)]$, $V_{OL1}(x,y) = I_0\sin^2(kx)$ and $V_{OL2}(x,y) = I_0\cos^2(kx)$. k is the wave vector of the laser light used for the optical lattice potentials, and I_0 is the potential depth of the lattices [37,41,42].

To obtain the real ground-state, we start from proper initial wave-functions and use the imaginary-time propagation approach. The lowest-energy states in different parameter space are obtained until the fluctuation in the norm of the wave function becomes smaller than 10^{-6} [43,44]. Here we want to note that for component 2, the *effective* contact interactions between atoms can be controlled by modifying atomic collisions (achieved by magnetically tuning the Feshbach resonances), or the atom number N; while for dipolar component 1, the most important quantity is the relative strength between the dipolar and contact interactions. Without loss of generality, in the following numerical simulations, we consider the special case with $N_1 = N_2 = N$, $\Omega_1 = \Omega_2 = \Omega$, and $g_{11} = g_{22} = g_{21} = g_{12} = g > 0$, and work in dimensional units by scaling with the trap energy $\hbar\omega_z$ and l_z where appropriate.

3. Numerical results and discussion

In what follows we will carry out a detailed numerical analysis of the combined effects of the DDI and rotation on the ground-state density distributions of the system. To highlight their effects, we further fix the contact interaction $g = 100$, the potential depth of the lattices $I_0 = 50$, and the period of the optical potential $T = \pi/3$. Fig. 1 shows the typical density profiles of a rotating two-component dipolar BEC in spin-dependent optical lattices, for rotation frequency $\Omega = 0.6$, and for a relatively small value of $\varepsilon_{dd} = 0.3$. As expected, in the presence of the spin-dependent optical lattices, the density distributions of the two components show phase separation, where the peak of each component corresponds to the minima of respective optical lattice. Consequently, it leads to the formation of alternately arranged stripes, as shown in Fig. 1(d) for the density difference of these two components [37,45,46].

More insights can be obtained if we look at the phase distributions of the two components, which are not shown here [the corresponding vortices are marked by crosses ($\times$)]. Remarkably, we observe that the vortices of each component are aligned in lines, and the system develops to an alternately arranged straight vortex sheet. Due to the system considered here is a two-component one, the positions of vortices of one component are vortex-free regions for the other one, thus the vortices observed here are called "coreless vortices". Here we notice that although these vortex structures have been discussed long time ago for helium systems and recently for cold atom gases, the effects of DDI on the two-component system considered here have not been studied as thoroughly.

On the other hand, we notice that a two-component system allows the existence of half-quantized vortices (winding number one half of a singly quantized vortex in scalar BECs). That is, when one travels around a vortex, the phase of one component rotates by 2π with the phase of the other component kept constant, and in this case, the *mass current* is rotated by π and the *spin current* by π or $-\pi$ [47]. Thus we **cautiously** refer to these vortices and its related vortex structures as half-quantized vortices and half-vortex sheets, respectively.

Another interesting observation is that the number of vortices of the central vortex sheet is different between these two components. More specifically, there are 2 (3) visible vortices for dipolar

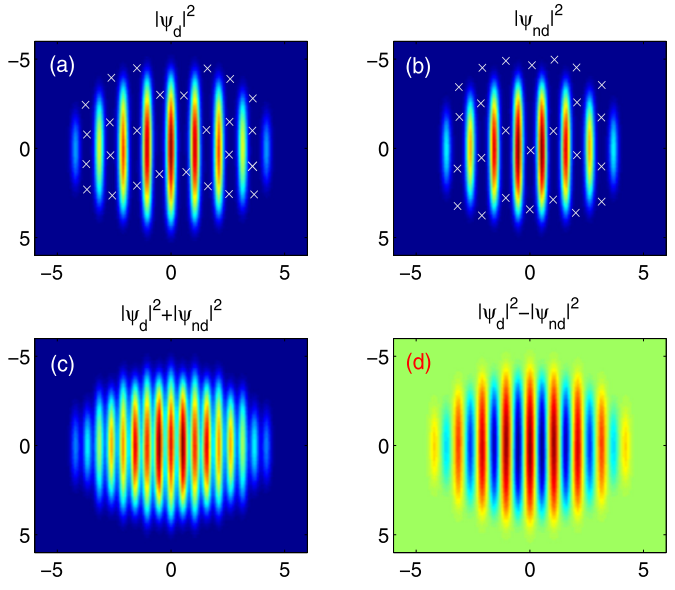

Fig. 1. (Color online.) Typical density profiles of a rotating two-component dipolar Bose–Einstein condensate in an optical lattice, for contact interactions $g = 100$, and for the rotation frequency $\Omega = 0.6$. Here the relative strength between the dipolar and contact interactions of component 1 is fixed to $\varepsilon_{dd} = 0.3$, (c) and (d) correspond to the total density and density difference of these two components, respectively. The locations of the vortices are marked by crosses (×).

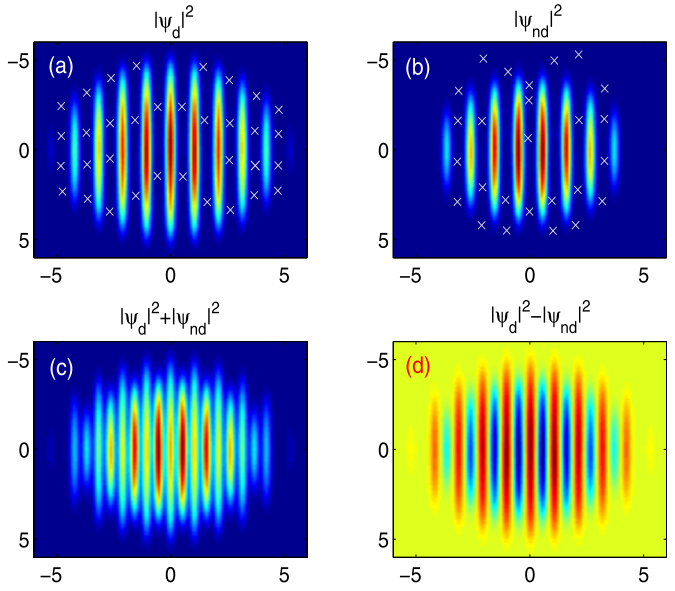

Fig. 2. (Color online.) Typical density profiles of a rotating two-component dipolar Bose–Einstein condensate in an optical lattice, for contact interactions $g = 100$, and for the rotation frequency $\Omega = 0.6$. Here the relative strength between the dipolar and contact interactions of component 1 is fixed to $\varepsilon_{dd} = 0.8$, (c) and (d) correspond to the total density and density difference of these two components, respectively. The locations of the vortices are marked by crosses (×).

(non-dipolar) component, as shown in Figs. 1(a) and (b). This phenomenon also appears in the following discussions, and in what follows we will give a more detailed physical explanation.

Increasing the strength of ε_{dd} to 0.8, it is found that the number of vortices increases with the increase of ε_{dd}. Typical density profiles of such a situation is shown in Fig. 2 for a larger value of $\varepsilon_{dd} = 0.8$. As shown in this figure, it is easy to see that the number of vortex sheet of the dipolar component increases from 8 for $\varepsilon_{dd} = 0.3$ to 10 for $\varepsilon_{dd} = 0.8$. In this case, to meet the requirement that the sheets should accommodate all the vortices (including the new nucleated one), 2 newly-formed vortex sheet appear to accommodate the new nucleated vortices [31]. From the above analysis, it is not difficult to speculate that with further increase of ε_{dd}, more and more vortices will appear, and the *effectively* repulsive contact interaction for dipolar component is further increased, leading to further expansion of the dipolar cloud.

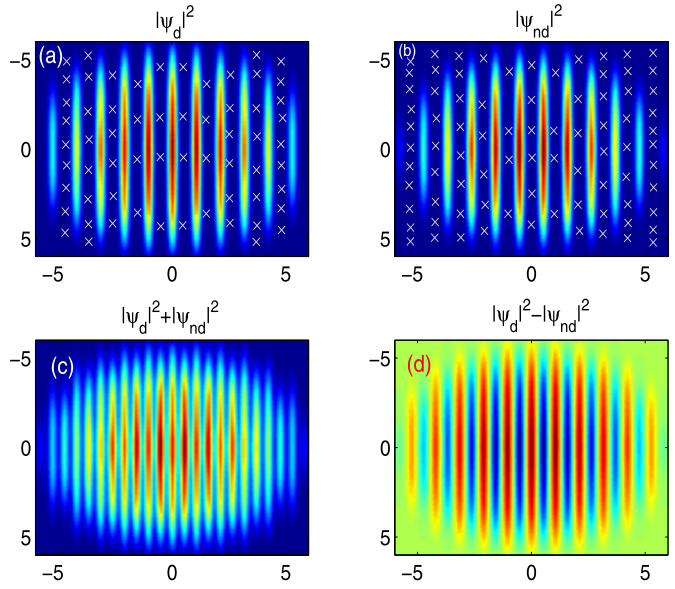

Fig. 3. (Color online.) Typical density profiles of a rotating two-component dipolar Bose–Einstein condensate in an optical lattice, for contact interactions $g = 100$, and for a higher rotation frequency $\Omega = 0.9$. Here the relative strength between the dipolar and contact interactions of component 1 is fixed to $\varepsilon_{dd} = 0.3$, (c) and (d) correspond to the total density and density difference of these two components, respectively. The locations of the vortices are marked by crosses (×).

All the above observed vortex structures can be understood by the simple physics that vortices always appear in the low-density regions to lower the total energy of the system. On the other hand, due to the dipoles are polarized along the symmetry axis of the harmonic potential, the DDI in this special case is purely repulsive and isotropic. The dipolar atoms which have kinetic energies high enough that they can overcome the trapping potential and occupy the outside regime. Consequently, the inclusion of DDI introduces another "switch", which can be used not only to obtain the desired ground-state phase, but also to control the number of vortices and its related vortex structures, even for a non-dipolar condensate.

It is also instructive to study the effects of rotation on the ground-state vortex structure of the system. Fig. 3 exhibits the typical density profiles of the system for fixed $g = 100$ and $\varepsilon_{dd} = 0.3$, but for a higher rotation frequency $\Omega = 0.9$. As before, the system again develops to the coreless–vortex structure, and the number of vortices increases with the increase of the rotation frequency. In addition, due to the large centrifugal force associated with the rotation, the dipolar component has a more larger expansion area.

To estimate the experimental feasibility of the proposed vortex structures, we notice that this special two-component system can be realized by selecting two states in the ground hyperfine manifolds of atomic Cr, Er, or Dy, where components 1 and 2 consist of states with spin projections $m_J = -J$ and $m_J = 0$. With regard to the interaction parameters, typically, ^{52}Cr with magnetic dipole moment $d = 6\mu_B$ and s-wave scattering length $a \approx 100a_0$ (here a_0 is the Bohr radius), the relative strength between the DDI and contact interaction $\varepsilon_{dd} = 0.036$ [48]. However, in realistic physical systems, the contact interactions g can be controlled by modifying the atomic collisions, which are experimentally feasible due to the flexible and precise control of the scattering length achievable by tuning the Feshbach resonance, making the DDI dominant.

In addition, the potential depth of the lattices I_0 can be precisely controlled by optics means, which scales with the laser's intensity [49]. Consequently, the parameters used in this study are within current experimental capacity.

Before the conclusion, we would like to emphasize that while the numerical results presented above are restricted to some particular parameter values, we also have conducted extensive numerical simulations over a range of different parameter sets, and found that the parameter sets selected here illustrate well the possible vortex structures. In addition, while this work is limited to magnetic DDI, the numerical method we present here is general for all dipolar quantum gases and may be employed in calculating the effects of electric DDI as well. Due to the anisotropic nature of the DDI, further work can be extended to a more general situation where the orientation of the dipoles can also be regarded as another "degree of freeedom" and more interesting phenomena, such as fractionalized skyrmion and topological spin texture, can occur.

4. Conclusions

To conclude, we have investigated the ground-state vortex structures of a rotating two-component dipolar BEC, which consists of both dipolar and scalar bosonic atoms, in spin-dependent optical lattices. At the mean-field level, the ground state densities of the system are studied as a function of the relative strength between the dipolar and contact interactions, and of the rotation frequency. From the preceding results, it is clear that the DDI and rotation, worked as effective "switches", can be used not only to obtain the desired ground-state phase, but also to control the number of vortices and its related vortex structures. The results not only help us better understand the effects of DDI and rotation on the ground-state vortex structures, but also offer us an effective way to manipulate this coupled dipolar BEC in future experiments. Finally, such a type of vortex structure is within the reach of current experiments with ultracold atoms.

Acknowledgements

This work was supported by NSF of China under Grants No. 61025023, No. 11303030, and No. 11565021; the NMFSEID under Grant No. 61127901. X.F. Zhang is also supported by the Chinese Academy of Sciences Key Project "Light of West China" Program under Grant No. 2012ZD02, the Science and Technology Project of Shaanxi Province under Grant No. 2013KJXX-03, and the Youth Innovation Promotion Association of the Chinese Academy of Sciences under Grant No. 2015334.

References

[1] S. Coen, M. Haelterman, Phys. Rev. Lett. 87 (2001) 140401.
[2] J.E. Williams, M.J. Holland, Nature 401 (1999) 568.
[3] J.R. Abo-Shaeer, C. Raman, J.M. Vogels, W. Ketterle, Science 292 (2001) 476.
[4] A.E. Leanhardt, Y. Shin, D. Kielpinski, D.E. Pritchard, W. Ketterle, Phys. Rev. Lett. 90 (2003) 140403.
[5] L.E. Sadler, J.M. Higbie, S.R. Leslie, M. Vengalattore, D.M. Stamper-Kurn, Nature 443 (2006) 312.
[6] J. Jin, S. Zhang, W. Han, J. Phys. B 44 (2011) 165302.
[7] M.H. Anderson, M.R. Matthews, C.E. Wieman, E.A. Cornell, Science 269 (1995) 198.
[8] K.B. Davis, M.O. Mewes, M.A. Joffe, M.R. Andrews, W. Ketterle, Phys. Rev. Lett. 74 (1995) 5202.
[9] K.B. Davis, M.O. Mewes, M.R. Andrews, N.J. van Druten, D.S. Durfee, D.M. Kurn, W. Ketterle, Phys. Rev. Lett. 75 (1995) 3969.
[10] F. Dalfovo, S. Giorgini, L.P. Pitaevskii, S. Stringari, Rev. Mod. Phys. 71 (1999) 463.
[11] A.J. Leggett, Rev. Mod. Phys. 73 (2001) 307.
[12] C.J. Pethick, H. Smith, Bose–Einstein Condensation in Dilute Gases, Cambridge University Press, Cambridge, UK, 2002.
[13] J. Stuhler, A. Griesmaier, T. Koch, M. Fattori, T. Pfau, S. Giovanazzi, P. Pedri, L. Santos, Phys. Rev. Lett. 95 (2005) 150406.
[14] A. Griesmaier, J. Werner, S. Hensler, J. Stuhler, T. Pfau, Phys. Rev. Lett. 94 (2005) 160401.
[15] T. Lahaye, T. Koch, B. Frohlich, M. Fattori, J. Metz, A. Griesmaier, S. Giovanazzi, T. Pfau, Nature 448 (2007) 672.
[16] T. Koch, T. Lahaye, J. Metz, B. Frohlich, A. Griesmaier, T. Pfau, Nat. Phys. 4 (2008) 218.
[17] K. Aikawa, A. Frisch, M. Mark, S. Baier, A. Rietzler, R. Grimm, F. Ferlaino, Phys. Rev. Lett. 108 (2012) 210401.
[18] J.J. McClelland, J.L. Hanssen, Phys. Rev. Lett. 96 (2006) 143005.
[19] M. Lu, H. Youn, B.L. Lev, Phys. Rev. Lett. 104 (2010) 063001;
M. Lu, N.Q. Burdick Seo, H. Youn, B.L. Lev, Phys. Rev. Lett. 107 (2011) 190401.
[20] N.R. Cooper, Adv. Phys. 57 (2008) 539.
[21] M.A. Baranov, Phys. Rep. 464 (2008) 71.
[22] I. Bloch, J. Dalibard, W. Zwerger, Rev. Mod. Phys. 80 (2008) 885.
[23] A.L. Fetter, Rev. Mod. Phys. 81 (2009) 647.
[24] T. Lahaye, C. Menotti, L. Santos, M. Lewenstein, T. Pfau, Rep. Prog. Phys. 72 (2009) 126401.
[25] C. Chin, R. Grimm, P. Julienne, E. Tiesinga, Rev. Mod. Phys. 82 (2010) 1225.
[26] J. Werner, A. Griesmaier, S. Hensler, J. Stuhler, T. Pfau, A. Simoni, E. Tiesinga, Phys. Rev. Lett. 94 (2005) 183201.
[27] S.B. Papp, J.M. Pino, C.E. Wieman, Phys. Rev. Lett. 101 (2008) 040402.
[28] W.E. Shirley, B.M. Anderson, C.W. Clark, R.M. Wilson, Phys. Rev. Lett. 113 (2014) 165301.
[29] B.C. Mulkerin, R.M.W. van Bijnen, D.H.J. O' Dell, A.M. Martin, N.G. Parker, Phys. Rev. Lett. 111 (2013) 170402.
[30] X.F. Zhang, W. Han, L. Wen, P. Zhang, R.F. Dong, H. Chang, S.G. Zhang, Sci. Rep. 5 (2015) 8684.
[31] Y. Zhao, J. An, C.D. Gong, Phys. Rev. A 87 (2013) 013605.
[32] E.Ö. Karabulut, F. Malet, G.M. Kavoulakis, S.M. Reimann, Phys. Rev. A 87 (2013) 033615.
[33] K.T. Xi, J. Li, D.N. Shi, Phys. Rev. A 84 (2011) 013619.
[34] T. Sowiński, O. Dutta, P. Hauke, L. Tagliacozzo, M. Lewenstein, Phys. Rev. Lett. 108 (2012) 115301.
[35] A. Chotia, B. Neyenhuis, S.A. Moses, B. Yan, J.P. Covey, M. Foss-Feig, A.M. Rey, D.S. Jin, J. Ye, Phys. Rev. Lett. 108 (2012) 080405.
[36] J. Deiglmayr, Phys. Rev. Lett. 101 (2008) 133004.
[37] W. Han, S.Y. Zhang, J.J. Jin, W.M. Liu, Phys. Rev. A 85 (2012) 043626.
[38] A.J. Olson, D.L. Whitenack, Y.P. Chen, Phys. Rev. A 88 (2013) 043609.
[39] S.K. Adhikari, Phys. Rev. A 89 (2014) 013630.
[40] P. Pedri, L. Santos, Phys. Rev. Lett. 95 (2005) 200404.
[41] O. Mandel, M. Greiner, A. Widera, T. Rom, T.W. Hänsch, I. Bloch, Nature 425 (2003) 937.
[42] O. Mandel, M. Greiner, A. Widera, T. Rom, T.W. Hänsch, I. Bloch, Phys. Rev. Lett. 91 (2003) 010407.
[43] W. Bao, Y. Cai, H. Wang, J. Comput. Phys. 229 (2010) 7874.
[44] J.C. Cremon, G.M. Bruun, S.M. Reimann, Phys. Rev. Lett. 105 (2010) 255301.
[45] X.F. Zhang, Z.J. Du, R.B. Tan, R.F. Dong, H. Chang, S.G. Zhang, Ann. Phys. 346 (2014) 154.
[46] K. Kasamatsu, M. Tsubota, M. Ueda, Phys. Rev. Lett. 91 (2003) 150406.
[47] M. Eto, K. Kasamatsu, M. Nitta, H. Takeuchi, M. Tsubota, Phys. Rev. A 83 (2011) 063603.
[48] I. Tikhonenkov, B.A. Malomed, A. Vardi, Phys. Rev. Lett. 100 (2008) 090406.
[49] S. Burger, F.S. Cataliotti, C. Fort, F. Minardi, M. Inguscio, M.L. Chiofalo, M.P. Tosi, Phys. Rev. Lett. 86 (2001) 4447.